Outer- and inner-valence ionization spectra of NH_3, PH_3, and AsH_3: symmetry-adapted cluster configuration interaction general-*R* study

Mayumi Ishida, Masahiro Ehara, and Hiroshi Nakatsuji[a)]
Department of Synthetic Chemistry and Biological Chemistry, Graduate School of Engineering, Kyoto University, Sakyou-ku, Kyoto 606-8501, Japan

(Received 23 August 2001; accepted 6 November 2001)

Outer- and inner-valence ionization spectra of group V hydrides, NH_3, PH_3, and AsH_3 were studied by the symmetry-adapted-cluster configuration-interaction (SAC-CI) general-*R* method. Fine details of the experimental spectra of these hydrides were reproduced and the quantitative assignments of the peaks were proposed. The inner-valence satellites were classified into those including the valence or Rydberg excitations. For NH_3, we interpreted the spectrum using the relative intensity and proposed some unresolved bands. For PH_3, bands 2 and 3, for which different assignments have been proposed, were attributed to the $^2A_1$ inner-valence satellites. A detailed inner-valence satellite spectrum of AsH_3 is theoretically proposed. © *2002 American Institute of Physics.*
[DOI: 10.1063/1.1430738]

I. INTRODUCTION

Many satellite peaks are usually involved in the inner-valence region of the ionization spectrum. They attracted considerable experimental and theoretical interests since they often provide information concerning electron correlations in molecules. Recently, extensive experimental studies of these peaks have been performed by the high-resolution synchrotron radiation photoelectron spectroscopy (SRPES), x-ray photoelectron spectroscopy (PES), and electron momentum spectroscopy (EMS). In parallel, advanced theoretical methods have also been used for detailed and quantitative assignments of these peaks.

The inner-valence regions of the group V hydrides, NH_3, PH_3, and AsH_3 provide an interesting target for these spectroscopies, and actually many satellite peaks with complicated band structures have been observed. Though early experimental works using He I and II PES (Refs. 1, 2) were rather limited in the study of the outer-valence region, careful and detailed studies on the inner-valence satellite peaks have been performed for NH_3 and PH_3 by He II PES,[3] SRPES,[4–6] EMS,[7,8] and $(e,2e)$ experiments.[9,10] So far, no experimental information on the inner-valence ionization spectrum of AsH_3 is available.

Theoretically, the outer- and inner-valence ionization spectra of these hydrides have been investigated by the multireference singles and doubles configuration-iteration (MR-SDCI) method,[7,8,11,12] the Green's function method,[8,13–15] and the $3h-2p-1p$ CI method.[16] However, since the satellite peaks are both numerous and complicated especially for PH_3, the detailed assignment in the inner-valence region is still difficult. It is important to perform fine and detailed calculations using extended basis sets and more reliable and accurate theoretical method including sufficient electron correlations, especially for the assignment of the high-lying shake-up states.

In this report, we studied the ionization spectra of NH_3, PH_3, and AsH_3 in the outer- and inner-valence regions using the symmetry-adapted-cluster (SAC) configuration-interaction (CI) general-*R* method. The SAC/SAC-CI method[17–19] has been successfully applied to molecular spectroscopic problems including ionization spectroscopy.[20–24,28–31] In particular, the SAC-CI general-*R* method[25–27] is designed to describe multi-electron processes with high accuracy, and has been shown to be useful for studying the large number of states appearing in the ionization spectrum.[28–31] In the SAC-CI general-*R* method, not only singles and doubles but also triples, quadruples, and higher-excitation operators are included as the linked excitation operators (R). Recently, we have given a fine analysis of the outer- and inner-valence ionization spectrum of group VI hydrides, H_2O, H_2S, and H_2Se.[31] Details of the SAC-CI general-*R* method can be found in Ref. 25 and in a review article recently summarized.[27]

Computational details are given in Sec. II, the results and discussions in Sec. III, and the concluding remarks in Sec. IV.

II. COMPUTATIONAL DETAILS

We studied vertical ionization spectra of NH_3, PH_3, and AsH_3 and the experimental geometries[32,33] were adopted; for NH_3 $R_{NH}=1.017$ Å and $\angle HNH=107.8°$, for PH_3 $R_{PH}=1.421$ Å, and $\angle HPH=93.3°$, and for AsH_3 $R_{AsH}=1.511$ Å and $\angle HAsH=92.1°$. We used valence triple-zeta (VTZ) basis sets of Ahlrichs,[34] augmented with three *d*-type and one *f*-type polarization functions of $\zeta_d=1.968$, 0.652, 0.216, $\zeta_f=0.452$ for P, two *d*-type polarization functions of $\zeta_d=1.654$, 0.469 for N, $\zeta_d=0.513$, 0.189 for As, and one *p*-type polarization function of $\zeta_p=0.8$ (Ref. 34) for H. The exponents of the polarization functions of N, P, and As were

a)Electronic mail: hiroshi@sbchem.kyoto-u.ac.jp

TABLE I. The SAC-CI general-*R* dimensions for calculating the ionized states of NH_3, PH_3, and AsH_3.

	State						
	C_s	C_{3v}	Singles	Doubles	Triples	Quadruples	Total
After perturbation selection							
NH_3	$^2A'$	$^2A_1+{}^2E$	3	560	35871	81024	117458
	$^2A''$	$^2A_2+{}^2E$	1	473	31038	56745	88257
PH_3	$^2A'$	$^2A_1+{}^2E$	3	669	42443	56845	99960
	$^2A''$	$^2A_2+{}^2E$	1	582	36220	40842	77645
AsH_3	$^2A'$	$^2A_1+{}^2E$	6	2824	34804	80771	118405
	$^2A''$	$^2A_2+{}^2E$	3	2525	25173	58158	85859
Before perturbation selection							
NH_3	$^2A'$	$^2A_1+{}^2E$	3	562	46663	1950844	1998072
	$^2A''$	$^2A_2+{}^2E$	1	478	46157	1951236	1997872
PH_3	$^2A'$	$^2A_1+{}^2E$	3	688	70648	3643076	3714415
	$^2A''$	$^2A_2+{}^2E$	1	592	69992	3643884	3714469
AsH_3	$^2A'$	$^2A_1+{}^2E$	6	3060	751060	99351960	100106086
	$^2A''$	$^2A_2+{}^2E$	3	2853	748652	99356376	100107884

taken from the correlation-consistent polarized VTZ (cc-pVTZ) sets[35,36] and the *d*-type function of $\zeta_d=1.968$ for P was determined by the extrapolation of other *d*-type functions. In addition, three *s*-, *p*-, and *d*-type Rydberg functions were put on N, P, and As atoms: $\zeta_s=0.039$, 0.012, 0.0037, $\zeta_p=0.041$, 0.013, 0.0041, $\zeta_d=0.133$, 0.038, 0.011 for N, $\zeta_s=0.039$, 0.012, 0.0038, $\zeta_p=0.036$, 0.013, 0.0046, $\zeta_d=0.071$, 0.024, 0.0078 for P, and $\zeta_s=0.038$, 0.012, 0.0041, $\zeta_p=0.057$, 0.022, 0.0082, $\zeta_d=0.060$, 0.022, 0.008 for As. The exponents of these Rydberg functions were determined by extrapolating the adopted basis sets. The resultant basis sets are $(13s9p5d)/[9s6p5d]$ for N, $(15s12p6d1f)/[10s8p6d1f]$ for P, $(17s14p10d)/[11s9p7d]$ for As, and $(5s1p)/[3s1p]$ for H, respectively.

The ionization spectra of NH_3, PH_3, and AsH_3 were calculated by the SAC-CI general-*R* method in both outer- and inner-valence regions up to around double-ionization threshold. These hydrides belong to the C_{3v} point group but the calculations were performed in the C_s point group. Most shake-up states of these hydrides were dominantly described by two-electron processes, and therefore the *R*-operators were included up to quadruples. The active space consists of 4 occupied and 65 unoccupied MOs for NH_3, 4 occupied and 80 unoccupied MOs for PH_3, and 9 occupied and 73 unoccupied MOs for AsH_3; the 1*s* orbital of N, 1*s*, 2*s*, and 2*p* orbitals of P, and 1*s*, 2*s*, 3*s*, 2*p*, and 3*p* orbitals of As were frozen as cores.

To reduce computational efforts, perturbation selection[21] was carried out in the state-selection scheme. For the ground state, the threshold for the linked operator was $\lambda_g=1\times10^{-8}$ a.u. and the unlinked terms were written as the products of the important linked terms whose SDCI coefficients were larger than 0.005. For the ionized states, the threshold for the double excitation operators was $\lambda_e=1\times10^{-7}$ a.u., that for triples was $\lambda_e=1\times10^{-6}$ a.u., and that for quadruples was $\lambda_e=5\times10^{-6}$ a.u. for NH_3 and PH_3 and $\lambda_e=1\times10^{-5}$ a.u. for AsH_3. The thresholds of the CI coefficients for calculating the unlinked operators in the SAC-CI method were 0.01 and 1×10^{-8} for the *R* and *S* operators, respectively.

The ionization cross-sections were calculated using the monopole approximation[37,38] to estimate the relative intensities of the peaks. In calculating monopole intensity, the correlated SAC wave function was used for the ground state; namely, both initial- and final-state correlation effects were included. In particular, the intensity of the $^2A_2$ state arises only from the initial-state correlation effect.

Hartree–Fock (HF) SCF calculations were performed using GAUSSIAN 98 (Ref. 39) and SAC/SAC-CI calculations were performed using the SAC-CI96 program system.[40]

III. RESULTS AND DISCUSSIONS

A. NH_3

The outer- and inner-valence ionization spectra of NH_3 up to 44 eV were studied by the SAC-CI general-*R* method. The SAC-CI calculations were performed in C_s, therefore, the $^2A_1$ and ^2E states of C_{3v} were calculated by $^2A'$ states of C_s, while the $^2A_2$ and ^2E states of C_{3v} were obtained by $^2A''$ states of C_s. To give theoretical assignments in the energy region up to 44 eV, 120 and 50 ionized states were calculated for $^2A'$ and $^2A''$ symmetries of C_s point group, respectively. Note that the shake-up states with considerable intensities were associated with $^2A_1$ symmetry. The SAC-CI general-*R* dimensions are summarized in Table I, together with those before the perturbation selection. Since most of the shake-up states were described predominantly by two-electron process, the SD-CI solutions were used for the reference states in the perturbation selection. The resultant dimensions were 117 458 and 88 257 for $^2A'$ and $^2A''$ symmetries, respectively.

The HF electronic configuration of NH_3 is written as $(\text{core})^2(2a_1)^2(1e)^4(3a_1)^2$.

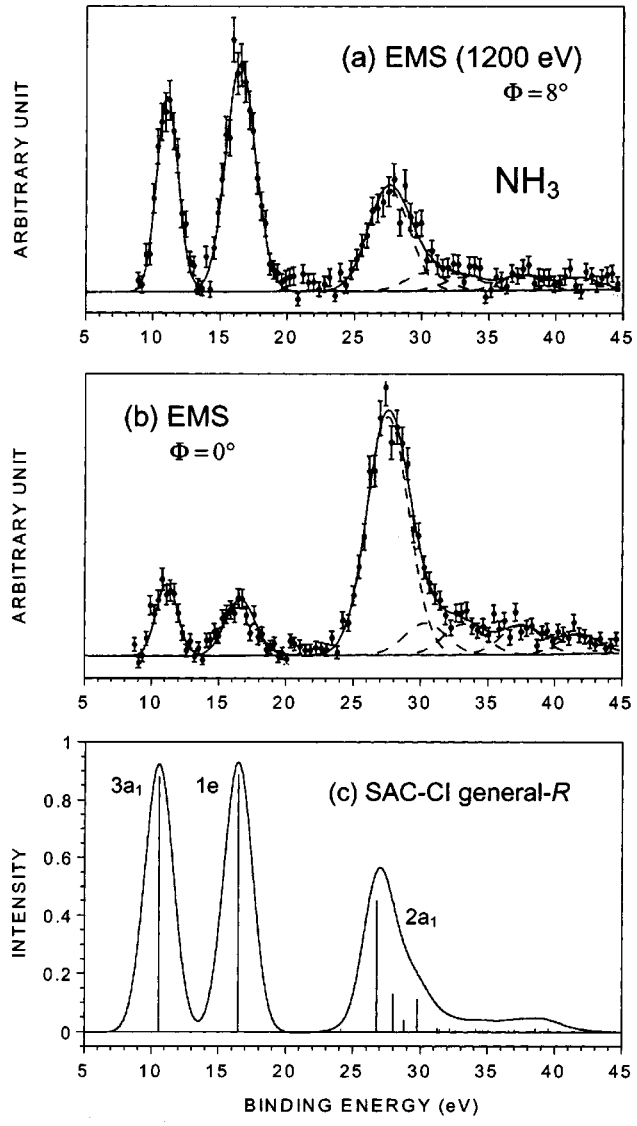

FIG. 1. The valence ionization spectra of NH_3 by (a) EMS at $\phi=8$ (Ref. 7), (b) EMS at $\phi=0$ (Ref. 7), and (c) the SAC-CI general-*R* method. In the theoretical spectrum, the calculated pole strength of each peak is convoluted with a FWHM of 3.6 eV.

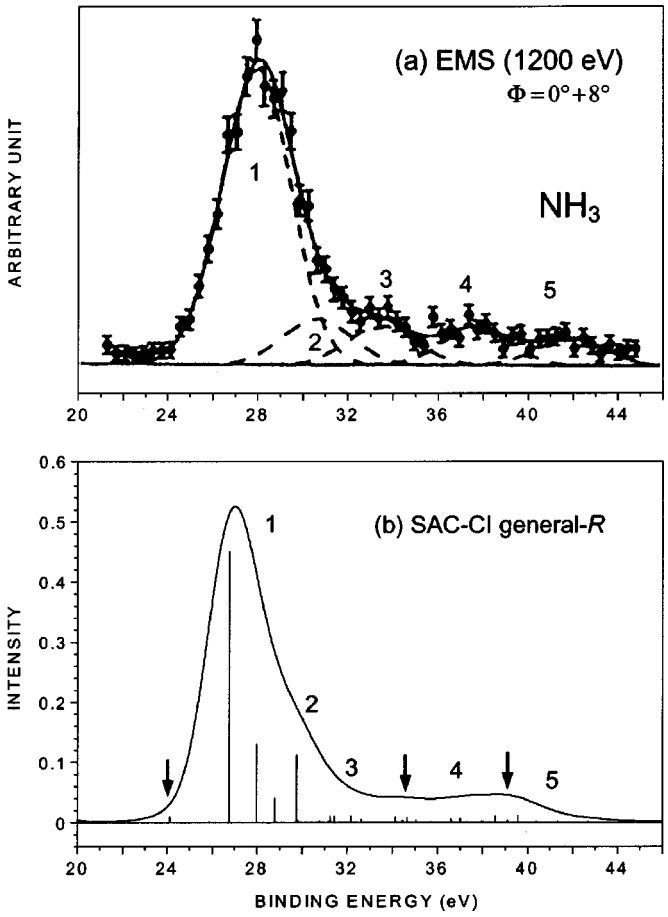

FIG. 2. The inner-valence ionization spectra of NH_3 by (a) EMS at $\phi=0+8$ (Ref. 7) and (b) the SAC-CI general-*R* method. In the theoretical spectrum, the calculated pole strength of each peak is shown as a solid vertical line and is convoluted with a FWHM of 3.6 eV. Arrows show additional predicted bands by the SAC-CI general-*R* method.

Figure 1 shows the ionization spectrum of NH_3 in the outer- and inner-valence regions calculated by the SAC-CI general-*R* method in comparison with the EMS spectra[7] at relative azimuthal angles ϕ of 0° and 8°. In the theoretical spectrum, the calculated pole strengths were shown by solid lines and were convoluted using Gaussian envelope with the FWHM of 3.6 eV. The theoretical spectrum reproduces both the main peaks and the satellites observed by the EMS quite accurately. First, we discuss two main peaks: $(3a_1^{-1})$ and $(1e^{-1})$ states, whose positions were precisely determined by the high-resolution PES using He I and II sources.[1,2] Table II gives the results for these peaks with the experimental IPs by EMS,[7] He II PES,[1] and He I PES.[2] Though there are some discrepancies in the experimental IPs, the SAC-CI general-*R* results, 10.57 and 16.46 eV, compare well with the experimental values of 10.85 and 16.4 eV (EMS), 10.88 and 16.0 eV (He II PES), and 10.85 and 16.5 eV (He I PES), for $(3a_1^{-1})$ and $(1e^{-1})$ states, respectively.

Next, the satellite peaks in the inner-valence region are discussed. The detailed satellite spectrum including the $(2a_1^{-1})$ inner-valence states was observed by the high-momentum-resolution EMS.[7] In Fig. 2, the inner-valence satellite spectrum by the present calculation is compared with EMS,[7] in which $\phi=0°$ and $\phi=8°$ spectra above 21 eV were summed and were deconvoluted with Gaussian functions (3.6 eV FWHM) as shown by the dashed lines. Our theoretical spectrum was also convoluted with the FWHM equal to a width of the EMS spectrum. Table II summarizes the IPs, monopole intensities, and main configurations of the inner-valence satellite peaks, whose IPs are up to 44 eV with intensities greater than 0.003. The outer-valence satellites accompanied by $(1e^{-1})$ are also given, though most of them are calculated to have very low intensities. The relative pole strengths were determined by the EMS for each azimuthal angles,[7] and were given in the parentheses.

Five satellite bands numbered 1–5 were observed by EMS. Three $^2A_1$ states calculated at 26.76, 27.98, and 28.79 eV are assigned to the strong band observed at 27.6 eV (band 1). The total pole strength of these states is calculated to be 0.623. These states are mainly described by a linear combination of $(2a_1^{-1})$ and two-electron processes such as $(3a_1^{-1}9e1e^{-1})$ and $(3a_1^{-2}na_1)$, which involve the excita-

TABLE II. Ionization potentials (IPs) (in eV), monopole intensities, and main configurations of the outer- and inner-valence ionized states of NH_3 calculated by the SAC-CI general-*R* method.

EMS[a]		PES[b]	PES[c]	SAC-CI general-*R*			
No.	IP	IP	IP	IP	Intensity[d]	State	Main configurations ($\|C\|>0.3$)
	10.85	10.88	10.85	10.57	0.880	$^2A_1$	$0.94(3a_1^{-1})$
	16.4	16.0	16.5	16.46	0.886	^2E	$0.95(1e^{-1})$
⋯	⋯	⋯	⋯	24.12	0.010	$^2A_1$	$0.60(3a_1^{-2}9a_1)-0.48(3a_1^{-2}12a_1)+0.40(3a_1^{-2}6a_1)$
⋯	⋯	⋯	⋯	25.88	0.001	^2E	$0.65(3a_1^{-2}9e)+0.46(3a_1^{-2}6e)$
1	27.6	27.0	⋯	26.76	0.451	$^2A_1$	$0.67(2a_1^{-1})-0.29(3a_1^{-1}9e1e^{-1})-0.28(3a_1^{-1}9e1e^{-1})$
	(1.00)			27.98	0.132	$^2A_1$	$0.36(2a_1^{-1})+0.58(3a_1^{-2}11a_1)+0.36(3a^{-2}8a_1)$
				28.79	0.040	$^2A_1$	$0.20(2a_1^{-1})+0.41(3a_1^{-1}9e1e^{-1})+0.40(3a_1^{-1}9e1e^{-1})+0.36(3a_1^{-2}10a_1)$
					(1.00)		
2	30.3	⋯	⋯	29.76	0.112	$^2A_1$	$0.33(2a_1^{-1})-0.44(3a_1^{-2}10a_1)-0.32(3a_1^{-2}11a_1)$
	(0.16)			29.81	0.004	$^2A_1$	$0.51(3a_1^{-2}8e)+0.36(3a_1^{-2}11e)-0.33(3a_1^{-2}7e)$
					(0.186)		
3	33.2	⋯	⋯	30.75	0.003	$^2A_1$	$0.54(3a_1^{-2}6a_1)+0.45(3a_1^{-2}4a_1)+0.36(3a_1^{-2}12a_1)$
	(0.13)			31.24	0.011	$^2A_1$	$0.33(1e^{-1}9e3a_1^{-1})+0.31(1e^{-1}9e3a_1^{-1})$
				31.43	0.011	$^2A_1$	$0.28(3a_1^{-2}8a_1)+0.27(1e^{-1}6e3a_1^{-1})-0.26(3a_1^{-1}7e1e^{-1})$
				32.17	0.011	$^2A_1$	$0.45(3a_1^{-2}8a_1)+0.44(3a_1^{-2}5a_1)-0.33(3a_1^{-2}11a_1)$
				32.61	0.006	$^2A_1$	$0.39(1e^{-1}7e3a_1^{-1})+0.38(1e^{-1}7e3a_1^{-1})$
				32.62	0.004	^2E	$0.51(3a_1^{-1}11a_11e^{-1})+0.42(3a_1^{-1}8a_11e^{-1})-0.38(3a_1^{-1}10a_11e^{-1})$ $-0.37(1e^{-1}10a_13a_1^{-1})$
					(0.074)		
⋯	⋯	⋯	⋯	34.12	0.010	$^2A_1$	$0.43(1e^{-1}8e3a_1^{-1})+0.39(1e^{-1}8e3a_1^{-1})-0.37(3a_1^{-2}8e)-0.32(3a_1^{-1}8e1e^{-1})$
				34.44	0.005	$^2A_1$	$0.26(3a_1^{-1}3e1e^{-1})+0.22(1e^{-2}6e)$
				34.49	0.003	$^2A_1$	$0.34(1e^{-2}9e)$
				34.66	0.009	$^2A_1$	$0.22(1e^{-2}9a_1)+0.22(1e^{-2}9a_1)$
				35.05	0.005	$^2A_1$	$0.56(3a_1^{-2}13a_1)+0.35(3a_1^{-2}10a_1)$
					(0.051)		
4	∼36.5[e]	⋯	⋯	36.59	0.007	$^2A_1$	$0.27(1e^{-2}9e)+0.26(1e^{-2}9e)$
	(0.13)			36.99	0.008	$^2A_1$	$0.45(3a_1^{-1}4e1e^{-1})+0.43(1e^{-1}4e3a_1^{-1})+0.36(3a_1^{-1}4e1e^{-1})$ $+0.35(1e^{-1}4e3a_1^{-1})$
				37.02	0.008	$^2A_1$	$0.36(1e^{-2}6e)+0.35(1e^{-2}9e)-0.34(1e^{-1}5a_13a^{-1})$
					(0.037)		
⋯	⋯	⋯	⋯	37.95	0.003	$^2A_1$	$0.26(3a_1^{-1}2e1e^{-1})+0.25(1e^{-1}2e3a_1^{-1})$
				38.56	0.011	$^2A_1$	$0.41(1e^{-2}7e)+0.38(1e^{-2}7e)+0.32(1e^{-2}10e)+0.30(1e^{-2}10e)$
				39.08	0.004	$^2A_1$	$0.52(1e^{-1}10e3a_1^{-1})-0.46(3a_1^{-1}11e1e^{-1})-0.42(1e^{-1}7e3a_1^{-1})$ $-0.37(3a_1^{-1}7e1e^{-1})+0.32(3a_1^{-1}10e1e^{-1})$
				39.11	0.004	$^2A_1$	$0.47(1e^{-1}10e3a_1^{-1})-0.43(3a_1^{-1}11e1e^{-1})-0.35(1e^{-1}7e3a_1^{-1})$ $-0.31(3a_1^{-1}7e1e^{-1})$
				39.56	0.013	$^2A_1$	$0.37(3a_1^{-1}11e1e^{-1})+0.36(3a_1^{-1}11e1e^{-1})$
					(0.056)		
5	41.8	⋯	⋯	41.32	0.003	$^2A_1$	$0.24(1e^{-2}6a_1)+0.24(1e^{-2}6a_1)+0.23(1e^{-2}12a_1)+0.22(1e^{-2}12a_1)$ $+0.22(1e^{-2}11a_1)$
	(0.10)						
					(0.016)		

[a](Ref. 7): the corresponding spectrum is shown in Figs. 1 and 2. Values in the parentheses are relative intensity to band 1.
[b]He II PES (Ref. 1).
[c]He I PES (Ref. 2).
[d]Values in the parentheses are relative intensity to band 1.
[e]This value is estimated by EMS (Ref. 7).

tions to valence anti-bonding orbital for two peaks at 26.76 and 28.79 eV, and those to Rydberg orbitals for a peak at 27.98 eV. Strong mixing of such configurations causes the split peak of band 1. He II PES also observed this satellite peak at 27 eV, and the MR-SDCI calculation[7] gave a state at 28.49 eV to this band. To band 2 observed at 30.3 eV, which is the shoulder of band 1, two $^2A_1$ states calculated at 29.76 and 29.81 eV are attributed. The former peak has the dominant intensity and the total pole strength of these states is calculated to be 0.116. As in the case of band 1, these states are characterized as the shake-up processes including Rydberg excitations. EMS reported the intensity of band 2 relative to band 1 as 0.16 ($\phi=0+8°$). Accordingly, our calculation gave a relative intensity of 0.19 for band 2.

Six continuous shake-up states calculated from 30.75 to 32.62 eV were attributed to the broadband deconvoluted at 33.2 eV (band 3). The total pole strength of these states was calculated to be 0.046. One of these shake-up states, calculated at 32.62 eV with an intensity of 0.004, is due to the $(1e^{-1})$ outer-valence satellite state. We also found a cluster of the states at around 34.5 eV, which consists of five $^2A_1$ states calculated at 34.12–35.05 eV with a total pole strength of 0.032. This band is also assigned to band 3 at 33.2 eV. The total pole strength of these eleven shake-up states from 30.75 to 35.05 eV is 0.078; the relative intensity is 0.125 in agreement with EMS value of 0.13. We consider that band 3 ac-

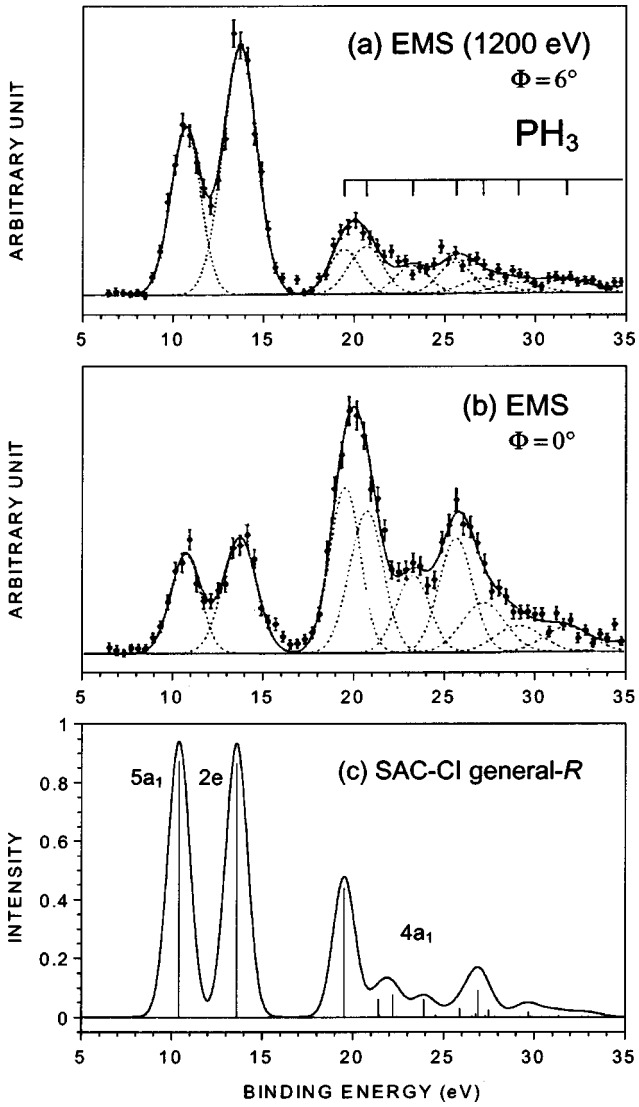

FIG. 3. The valence ionization spectra of PH_3 by (a) EMS at $\phi=6$ (Ref. 8), (b) EMS at $\phi=0$ (Ref. 8), and (c) the SAC-CI general-*R* method. In the theoretical spectrum, the calculated pole strength of each peak is convoluted with a FWHM of 2.0 eV.

tually consists of two bands. MR-SDCI also gave two peaks at 32.86 and 34.61 eV for band 3. Therefore, more detailed experimental study is necessary in this energy region.

In the EMS study, two weak broadbands 4 and 5 were observed at 36.5 and 41.8 eV, and these bands lay above the double-ionization threshold (33.7 ± 0.2 eV).[41] Though there are other possibilities for the assignments of these bands, we tentatively assign some shake-up states underlying in the continuum of the double ionized states. Three shake-up states from 36.59 to 37.02 eV with small intensities are attributed to band 4 around 36.5 eV. (Experimental IP of band 4 is estimated from the spectrum.) The total pole strength of these states amounts to 0.023. MR-SDCI also calculated the band 4 at 36.59 eV with a very small intensity. To band 5 observed at 41.8 eV, a shake-up state calculated at 41.32 eV is assigned. For this band, we actually obtained a number of states, whose intensities were less than 0.003 in the energy region of 40–44 eV, and a total pole strength of these states amounted to be 0.010. We also found a satellite band between bands 4 and 5. This band consists of five shake-up states with the total pole strength of 0.035. The relative intensity for the peaks of 35.5–44 eV was calculated to be 0.11, which is smaller than that of EMS, 0.23. However, the description in this energy region may be less accurate than other regions because double ionized states were not examined and the number of Rydberg orbitals included were limited. Neither the MR-SDCI (Ref. 7) nor the Green function method[13,14] extended into this energy region.

Finally, in the lower-energy region below the strong band 1, we found a weak peak at 24.12 eV though it was not reported by the experiment. This peak seems to correspond to the ''shake-down'' peak, as seen in the inner-valence satellite spectrum of the group VI hydrides.[31,42,43] MR-SDCI calculation also gave a weak peak at 26.32 eV. In this region, a $(1e^{-1})$ outer-valence satellite state was also calculated at 25.88 eV, although its intensity was very small, 0.001.

B. PH_3

Next, the SAC-CI general-*R* method was applied to the outer-and inner-valence ionization spectra of PH_3 up to about 34 eV. Adopting the C_s point group, 120 $^2A'$ and 50 $^2A''$ ionized states were calculated. The resultant SAC-CI general-*R* dimensions were 99 960 and 77 645 for $^2A'$ ($^2A_1+{}^2E$) and $^2A''$ ($^2A_2+{}^2E$) symmetries, respectively, as shown in Table I.

The HF electronic configuration of PH_3 was calculated as $(\text{core})^{10}(4a_1)^2(2e)^4(5a_1)^2$.

In Fig. 3, the SAC-CI ionization spectrum of PH_3 is compared with the EMS spectra[8] which were obtained at relative azimuthal angles ϕ of 0° and 6°. In the theoretical spectrum, the line widths of Gaussian convolution is 2.0 eV FWHM estimated from the EMS spectrum.[8] Table III summarizes the calculated IPs, monopole intensities, and main configurations together with the IPs by four experiments.[3,5,6,8,9] We presented the ionized states whose intensity was greater than 0.003, while we also gave some satellites with very small intensities, especially for the 19–23 eV region. Note that there are still several other outer- and inner-valence satellites that are not given in Table III. Unfortunately, there is no experimental information on the intensity for comparison.

Two main peaks due to $(5a_1^{-1})$ and $(2e^{-1})$ ionization processes were observed in the valence ionization spectrum of PH_3. The SAC-CI general-*R* method calculated these main peaks at 10.40 and 13.59 eV in accordance with the IPs by SRPES,[5,6] He II PES,[3] EMS,[8] and the binary $(e,2e)$ coincidence method,[9] as shown in Table III.

For the $(4a_1^{-1})$ inner-valence satellite peaks, we discuss the results comparing with the detailed spectrum by SRPES.[5,6] In Fig. 4, the inner-valence satellite spectrum of PH_3 calculated by the SAC-CI general-*R* method is shown along with the SRPES spectrum. In the theoretical spectrum, the calculated pole strengths are convoluted with the FWHM of 2.0 eV. Nine satellite bands 1–9 were observed up to 32 eV by SRPES. The spectrum of the correlation peaks of PH_3 is much more complicated than that of NH_3. The strongest peak (band 1) in the inner-valence region was observed at

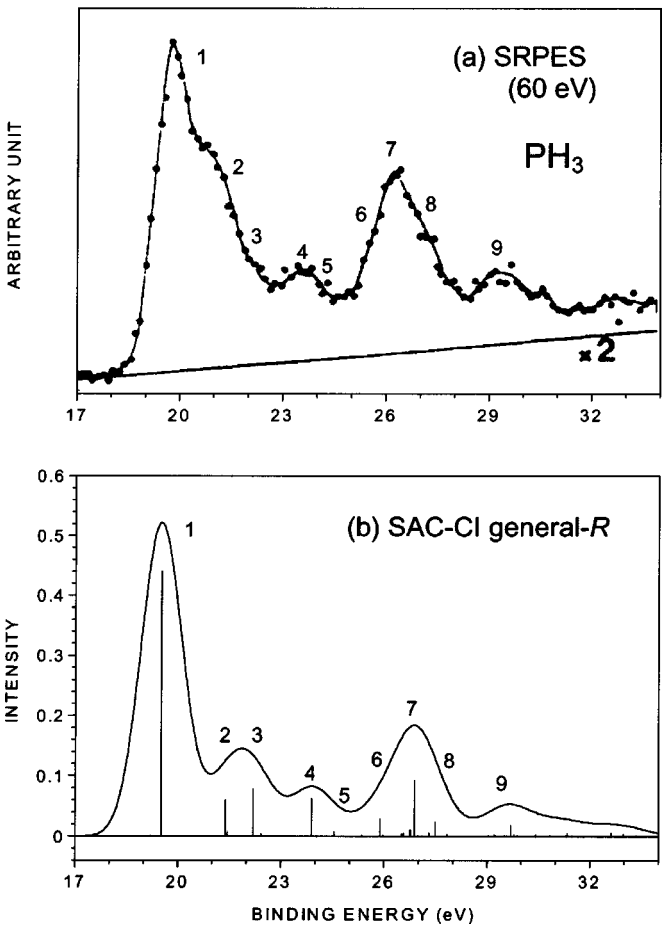

FIG. 4. The inner-valence ionization spectra of PH_3 by (a) SRPES (Refs. 5, 6), and (b) the SAC-CI general-*R* method. In the theoretical spectrum, the calculated pole strength of each peak is shown as a solid vertical line and is convoluted with a FWHM of 2.0 eV.

19.42 eV (SRPES), 19.5 eV (He II PES), 19.4 eV (EMS), and 19.45 eV [binary $(e,2e)$ coincidence method]. The SAC-CI general-*R* gave a strong peak at 19.52 eV with an intensity of 0.441 and well reproduced these experimental spectra. This state is described as a linear combination of $(4a_1^{-1})$ and shake-up states including valence-excitation, such as $(5a_1^{-1}10e2e^{-1})$ and $(2e^{-1}10e5a_1^{-1})$. In the simplified ADC(4),[8] this band was calculated at 19.28 eV, and in the MR-SDCI (Ref. 8) at 19.70 eV.

In the shoulder of band 1, two bands 2 and 3 were observed at 20.61 and 21.72 eV by SRPES. We assign a $^2A_1$ state calculated at 21.40 eV to band 2, and two $^2A_1$ states calculated at 22.20 and 22.43 eV to band 3. These states are characterized as the shake-up states accompanied by the valence-excitation like band 1. Different assignments have been proposed for these bands. Cauletti *et al.*[5,6] suggested that bands 2 and 3 were due to the outer-valence satellites on the basis of their results by β spectrum of SRPES. On the other hand, EMS observed a peak at 20.6 eV corresponding to band 2 and/or 3 and the binary $(e,2e)$ coincidence method also observed a peak at 22.61 eV. These peaks were analyzed as "*s*-type;" i.e., it was dominantly due to the $(4a_1^{-1})$ inner-valence satellite. In addition, the simplified ADC(4) calculation gave two $^2A_1$ states at 20.98 and 22.32 eV to bands 2 and 3, respectively. In our calculation, although some peaks with different symmetries (^2E or $^2A_2$) were also obtained in this region, their intensities were quite small; the $(2e^{-1})$ outer-valence satellite states were calculated at 21.45 and 22.47 eV with intensities of 0.009 and 0.0005, and two $^2A_2$ states were at 20.94 and 22.42 eV with 0.0001. (Note that their intensities are purely due to the initial-state correlation.) Therefore, we also suggest that bands 2 and 3 are dominantly due to the $(4a_1^{-1})$ inner-valence satellite states and support the EMS and ADC(4) assignments. For two $^2A_1$ states attributed to band 3, a mixing of the two-electron processes including the excitations to the Rydberg orbitals was found and the *d*-type Rydberg basis sets were important for describing these states.

In the energy region between the strong and medium peaks, two weak bands 4 and 5 were observed by SRPES. We assigned two $^2A_1$ states calculated at 23.90 and 24.56 eV to these two bands at 23.3 and 24.1 eV, respectively. These states are described by a linear combination of $(4a_1^{-1})$ and $(5a_1^{-2}na_1)$, and are characterized as two-electron process including transition to $3d$ Rydberg orbital for band 4.

The medium peak was observed at around 26 eV and was decomposed into three bands 6–8. For these bands, we assign several shake-up states in good agreement with experiment. Two $^2A_1$ states calculated at 25.36 and 25.89 eV are attributed to band 6 at 25.56 eV, one ^2E state at 26.51 eV, and four $^2A_1$ states at 26.57–26.89 eV are attributed to band 7 at 26.54 eV, and one ^2E state at 27.31 eV and two $^2A_1$ states at 27.49 and 27.83 eV are attributed to band 8 at 27.82 eV, respectively. Two $^2A_1$ states calculated at 26.57 and 26.89 eV, which are assigned to band 7, are described by a linear combination of $(4a_1^{-1})$ and two-electron processes including excitations to valence orbitals, such as $(5a_1^{-2}9a_1)$ and $(2e^{-2}10e)$. Other states are mainly due to the shake-up states involving Rydberg excitations. In this energy region, EMS observed two bands at 25.6 and 27.2 eV. The former band corresponds to bands 6 and 7 in SRPES, and the latter band corresponds to band 8. The binary $(e,2e)$ coincidence method observed only one band at 25.46 eV.

For band 9 observed at 29.12 eV, three $^2A_1$ states were calculated at 29.21, 29.69, and 29.79 eV, and were characterized as $(5a_1^{-1}ne2e^{-1})$ and $(2e^{-2}11e)$ including Rydberg excitations. In EMS, a weak band was observed at 31.8 eV. We assign one ^2E state at 30.42 eV and four $^2A_1$ states calculated at 30.84–32.98 eV to this band. Finally, in the satellite spectrum of PH_3, no "shake-down" peak, which borrows intensity from the $(4a_1^{-1})$ state, was calculated, and in this energy region, a $(2e^{-1})$ outer-valence satellite state was calculated at 19.20 eV with a small intensity.

C. AsH_3

The ionization spectrum of AsH_3 up to about 33 eV was studied in both the outer- and inner-valence regions, though the experimental observation has been limited only for the former region. As in NH_3 and PH_3, 120 and 50 states were examined for (A_1+E) and (A_2+E) symmetries, respec-

TABLE III. Ionization potentials (IPs) (in eV), monopole intensities, and main configurations of the outer- and inner-valence peaks of PH_3 calculated by the SAC-CI general-*R* method.

SRPES[a]		He II[b]	EMS[c]	$(e,2e)$[d]	SAC-CI general-*R*			
No.	IP	IP	IP	IP	IP	Intensity	State	Main configurations ($\|C\|>0.3$)
	10.59	10.58	10.6	10.59	10.40	0.873	$^2A_1$	$0.94(5a_1^{-1})$
	13.59	13.5	13.6	13.44	13.59	0.866	^2E	$0.93(2e^{-1})$
⋯	⋯	⋯	⋯	⋯	19.20	0.002	^2E	$0.76(5a_1^{-2}10e)-0.40(5a_1^{-2}7e)-0.30(5a_1^{-2}9e)$
1	19.42	19.5	19.4	19.45	19.52	0.441	$^2A_1$	$0.66(4a_1^{-1})-0.36(5a_1^{-1}10e2e^{-1})$ $-0.35(2e^{-1}10e5a_1^{-1})$
2	20.61	20.5	20.6	⋯	20.94	0.0001	$^2A_2$	$0.56(2e^{-1}10e5a_1^{-1})-0.53(2e^{-1}10e5a_1^{-1})$ $-0.34(2e^{-1}7e5a_1^{-1})+0.32(2e^{-1}7e5a_1^{-1})$
					21.40	0.061	$^2A_1$	$0.24(4a_1^{-1})+0.44(5a_1^{-2}12a_1)+0.34(5a_1^{-2}9a_1)$ $-0.34(5a_1^{-1}10e2e^{-1})$
					21.45	0.009	^2E	$0.49(2e^{-1}10e5a_1^{-1})+0.48(5a_1^{-1}10e2e^{-1})$ $-0.48(2e^{-1}10e5a_1^{-1})-0.37(5a_1^{-1}10e2e^{-1})$
3	21.72	⋯	⋯	22.61	22.20	0.078	$^2A_1$	$0.28(4a_1^{-1})+0.33(5a_1^{-2}12a_1)$ $+0.33(5a_1^{-2}14a_1)+0.31(2e^{-1}10e5a_1^{-1})$
					22.42	0.0001	$^2A_2$	$0.54(5a_1^{-1}10e2e^{-1})-0.41(5a_1^{-1}10e2e^{-1})$ $-0.37(5a_1^{-1}7e2e^{-1})$
					22.43	0.005	$^2A_1$	$0.33(5a_1^{-2}14a_1)$
					22.47	0.0005	^2E	$0.63(5a_1^{-1}5e2e^{-1})+0.61(2e^{-1}5e5a_1^{-1})$ $+0.43(5a_1^{-1}4e2e^{-1})+0.43(2e^{-1}5e5a_1^{-1})$
4	23.3	⋯	23.2	⋯	23.90	0.062	$^2A_1$	$0.24(4a_1^{-1})-0.49(5a_1^{-2}14a_1)-0.31(5a_1^{-2}11a_1)$
5	24.1	⋯	⋯	⋯	24.56	0.007	$^2A_1$	$0.60(5a_1^{-2}13a_1)+0.47(5a_1^{-2}10a_1)$
6	25.56	⋯	25.6	25.46	25.36	0.003	$^2A_1$	$0.67(5a_1^{-1}11e2e^{-1})+0.41(2e^{-1}11e5a_1^{-1})$ $-0.39(5a_1^{-1}8e2e^{-1})+0.31(5a_1^{-1}14e2e^{-1})$
					25.89	0.030	$^2A_1$	$0.40(2e^{-1}11e5a_1^{-1})+0.38(2e^{-1}11e5a_1^{-1})$ $-0.30(2e^{-1}8e5a_1^{-1})$
7	26.54	⋯	⋯	⋯	26.51	0.004	^2E	$0.31(5a_1^{-1}14a_12e^{-1})-0.31(2e^{-1}13a_15a_1^{-1})$
					26.57	0.006	$^2A_1$	$0.48(5a_1^{-2}9a_1)+0.45(5a_1^{-2}6a_1)$ $+0.45(5a_1^{-2}15a_1)$
					26.75	0.011	$^2A_1$	$0.54(2e^{-1}9e5a_1^{-1})+0.53(2e^{-1}6e5a_1^{-1})$ $+0.31(5a_1^{-1}9e2e^{-1})$
					26.77	0.012	$^2A_1$	$0.52(2e^{-1}9e5a_1^{-1})+0.50(2e^{-1}6e5a_1^{-1})$ $+0.34(5a_1^{-1}9e2e^{-1})$
					26.89	0.093	$^2A_1$	$0.29(4a_1^{-1})+0.34(2e^{-2}10e)+0.32(2e^{-2}10e)$
8	27.82	⋯	27.2	⋯	27.31	0.006	$^2E_1$	$0.61(5a_1^{-1}10a_12e^{-1})+0.60(5a_1^{-1}13a_12e^{-1})$ $+0.38(2e^{-1}13a_15a_1^{-1})$
					27.49	0.024	$^2A_1$	$0.55(5a_1^{-2}11a_1)+0.49(5a_1^{-2}8a_1)$ $-0.32(5a_1^{-2}14a_1)$
					27.83	0.004	$^2A_1$	$0.54(5a_1^{-2}7a_1)+0.44(5a_1^{-2}10a_1)$ $-0.42(5a_1^{-2}13a_1)$
9	29.12	⋯	29.1	⋯	29.21	0.003	$^2A_1$	$0.41(2e^{-1}7e5a_1^{-1})+0.37(5a_1^{-1}7e2e^{-1})$
					29.69	0.019	$^2A_1$	$0.40(5a_1^{-1}5e2e^{-1})-0.39(2e^{-2}11e)$ $+0.35(5a_1^{-1}8e2e^{-1})+0.33(2e^{-1}8e5a_1^{-1})$
					29.49	0.004	$^2A_1$	$0.38(5a_1^{-1}5e2e^{-1})+0.33(5a_1^{-1}8e2e^{-1})$ $+0.31(2e^{-1}8e5a_1^{-1})-0.30(2e^{-2}11e)$
⋯	⋯	⋯	31.8	⋯	30.42	0.003	^2E	$0.32(2e^{-2}9e)$
					30.84	0.003	$^2A_1$	$0.28(5a_1^{-1}12a_14a_1^{-1})+0.26(5a_1^{-1}3e2e^{-1})$ $+0.24(5a_1^{-1}3e2e^{-1})+0.22(5a_1^{-1}9a_14a_1^{-1})$
					31.35	0.006	$^2A_1$	$0.32(2e^{-2}14a_1)-0.30(2e^{-1}3e5a_1^{-1})$
					32.62	0.006	$^2A_1$	$0.50(5a_1^{-2}16a_1)-0.34(5a_1^{-2}7a_1)$ $-0.34(5a_1^{-2}14a_1)$
					32.98	0.004	$^2A_1$	$0.42(2e^{-2}7e)-0.40(2e^{-2}7e)$

[a]References 5, 6: the corresponding spectrum is shown in Fig. 4.
[b]Reference 3.
[c]Reference 8: the corresponding spectrum is shown in Fig. 3.
[d]The binary $(e,2e)$ coincidence method (Ref. 9).

tively. The SAC-CI general-*R* dimensions are given in Table I. Note that $3d$ orbitals of As were included in the active space.

The HF electronic configuration of AsH_3 was given by $(\text{core})^{18}\ (3e)^4\ (4e)^4\ (6a_1)^2\ (7a_1)^2\ (5e)^4\ (8a_1)^2$.

Figure 5 shows the valence ionization spectrum of AsH_3 by the SAC-CI general-*R* method, in comparison to that by the He II PES (~16 eV).[1] The calculated pole strengths were convoluted using Gaussian functions with the FWHM of 2.0 eV. In Table IV, the results for the main peaks of AsH_3 are summarized and compared with the He II PES IPs.[1] Two main peaks in the outer-valence region were well repro-

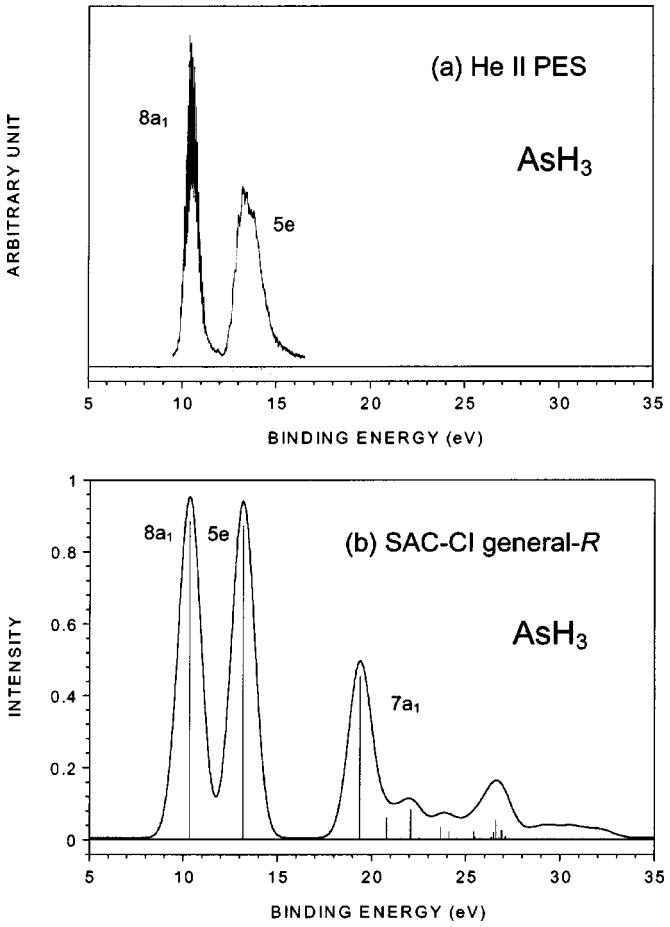

FIG. 5. The valence ionization spectra of AsH_3 by (a) He II PES (Ref. 1), and (b) the SAC-CI general-*R* method. In the theoretical spectrum, the calculated pole strength of each peak is shown as a solid vertical line and is convoluted with a FWHM of 2.0 eV.

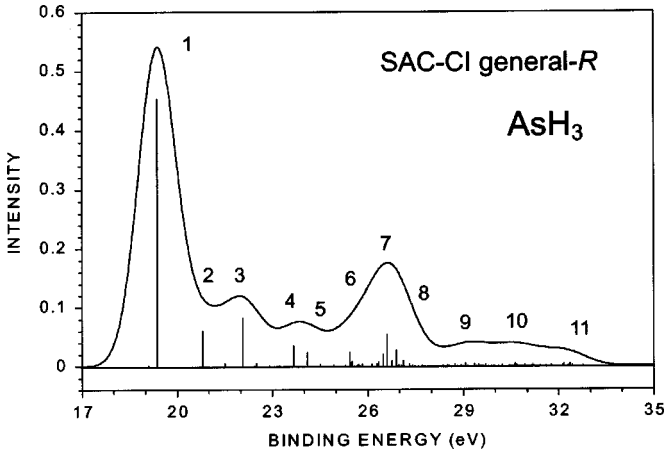

FIG. 6. The inner-valence ionization spectrum of AsH_3 by the SAC-CI general-*R* method. The calculated pole strength of each peak is convoluted with a FWHM of 2.0 eV. The eleven bands numbered 1–11 are evaluated by the convolution of the peaks.

duced; they were calculated at 10.32 and 13.17 eV for the $(8a_1^{-1})$ and $(5e^{-1})$ states, respectively, whose experimental IPs were reported as 10.51 and 13.2 eV by the He II PES.

To our knowledge, the experimental spectrum in the inner-valence region of AsH_3 has not yet been reported. Although only one band at 19.0 eV was given by the He II PES, this IP was deduced from those of other molecules. The valence ionization spectrum of this molecule was theoretically investigated by the $2h-1p$ and $3h-2v-1p$ CI methods.[12,16]

The satellite spectrum in the $(7a_1^{-1})$ inner-valence region of AsH_3 by the SAC-CI general-*R* method is presented in Fig. 6. Table IV also shows the results for the inner-valence satellite peaks of AsH_3. They are shown up to about 33 eV with the intensities greater than 0.003. From the present calculation, eleven satellite bands were found by the Gaussian convolution of the peaks, which were numbered 1–11 in the table. The spectrum shape of AsH_3 appears to be very similar to that of PH_3 as a whole.

The ''shake-down'' peak below the strong band was not calculated, while, in this energy region, the $(5e^{-1})$ outer-valence satellite state was obtained at 19.10 eV with a small intensity of 0.002, which is the same trend as PH_3. The $3h-2v-1p$ CI also did not calculate the peak in this region. In the case of H_2Se,[31] both the outer-valence satellite state and shake-down peak were found below the strong band.

The strong peak 1 was calculated at 19.38 eV, and was assigned to the band at 19.0 eV deduced in the He II PES work.[1] This state is mainly described by a linear combination of $(7a_1^{-1})$ and $(8a_1^{-1}12e5e^{-1})$, whose shake-up configuration includes excitations to the valence orbital.

Many shake-up states were found in the energy region of 20–33 eV, as in the case of NH_3 and PH_3. The main contribution to band 2 is from a $^2A_1$ state calculated at 20.81 eV with an intensity of 0.061, which is characterized as $(7a_1^{-1})$ and $(8a_1^{-2}na_1)$ including valence excitation. A $(5e^{-1})$ outer-valence satellite state at 21.51 eV is also attributed to band 2. Two $^2A_1$ states at 22.07 and 22.50 eV constitute band 3. The former state has dominant pole strength and is characterized as $(8a_1^{-1}12e5e^{-1})$ interacting with the $(7a_1^{-1})$. The total pole strength of these states is calculated to be 0.090.

Band 4 corresponds to a $^2A_1$ state calculated at 23.67 eV with the intensity of 0.035. Band 5 consists of four $^2A_1$ states and the intensity is dominantly from the state at 24.10 eV with the total pole strength being 0.033. Five $^2A_1$ states with the intensity from the state at 25.43 eV were attributed to band 6, a cluster of five $^2A_1$ states at 26.13–26.60 eV corresponds to band 7, and four $^2A_1$ states with two ^2E states at 26.75–27.31 eV were assigned as band 8. In the energy region from band 4 to 8, considerable mixing of the two-electron processes including excitations to the Rydberg orbitals is found. The *d*-type Rydberg basis sets were very important for describing these peaks, especially for bands 4, 6, 7, and 8.

In the energy region of 29–33 eV, three weak continuous bands 9–11 were predicted. Numerous states, whose intensities were less than 0.003, were also calculated in this region. Band 9 was composed of ~40 shake-up states from 27.7 to 30 eV with a total intensity of 0.045, band 10 was composed of ~30 states from 30 to 31.75 eV with a total intensity of 0.035, and band 11 was composed of ~15 states from 32 to 33 eV with a total intensity of 0.018, respectively. These

TABLE IV. Ionization potentials (IPs) (in eV), monopole intensities, and main configurations of the outer- and inner-valence peaks of AsH_3 calculated by the SAC-CI general-*R* method.

He II PES[a]	SAC-CI general-*R*				
IP	No.	IP	Intensity	State	Main configurations ($\|C\|>0.3$)
10.51		10.32	0.887	$^2A_1$	$0.94(8a_1^{-1})$
13.2		13.17	0.874	^2E	$0.93(5e^{-1})$
···		19.10	0.002	^2E	$0.71(8a_1^{-2}12e)+0.33(8a_1^{-2}10e)$
(19.0)	1	19.38	0.454	$^2A_1$	$0.67(7a_1^{-1})-0.36(8a_1^{-1}12e5e^{-1})-0.36(8a_1^{-1}12e5e^{-1})$
···	2	20.81	0.061	$^2A_1$	$0.55(8a_1^{-2}15a_1)+0.43(8a_1^{-2}12a_1)-0.32(8a_1^{-2}18a_1)$
		21.51	0.005	^2E	$0.53(5e^{-1}12e8a_1^{-1})-0.51(5e^{-1}12e8a_1^{-1})+0.40(8a_1^{-1}12e5e^{-1})-0.38(8a_1^{-1}12e5e^{-1})$
···	3	22.07	0.084	$^2A_1$	$0.43(8a_1^{-1}12e5e^{-1})+0.38(8a_1^{-1}12e5e^{-1})$
		22.50	0.006	$^2A_1$	$0.46(8a_1^{-2}16a_1)+0.39(5e^{-1}12e8a_1^{-1})+0.32(5e^{-1}12e8a_1^{-1})$
···	4	23.67	0.035	$^2A_1$	$0.43(8a_1^{-1}16a_1)+0.39(8a_1^{-2}14a_1)$
···	5	24.10	0.023	$^2A_1$	$0.54(8a_1^{-2}13a_1)+0.33(8a_1^{-2}17a_1)$
		24.11	0.003	$^2A_1$	$0.55(8a_1^{-2}9e)+0.39(8a_1^{-2}14e)+0.34(8a_1^{-2}6e)+0.32(8a_1^{-2}10e)$
		24.51	0.004	$^2A_1$	$0.44(5e^{-2}12e)+0.31(5e^{-1}15a_18a_1^{-1})+0.30(5e^{-1}12a_18a_1^{-1})$
		24.93	0.003	$^2A_1$	$0.54(5e^{-1}16a_18a_1^{-1})+0.32(5e^{-1}14a_18a_1^{-1})$
···	6	25.30	0.003	$^2A_1$	$0.37(5e^{-1}16a_18a_1^{-1})+0.33(8a_1^{-1}16a_15e^{-1})$
		25.43	0.024	$^2A_1$	$0.32(5e^{-2}13e)$
		25.49	0.008	$^2A_1$	$0.51(5e^{-2}13e)+0.38(5e^{-2}13e)-0.34(5e^{-2}11e)+0.30(5e^{-2}11e)$
		25.71	0.004	$^2A_1$	$0.39(8a_1^{-1}9e5e^{-1})+0.30(8a_1^{-1}14e5e^{-1})$
		25.82	0.004	$^2A_1$	$0.42(8a_1^{-2}9a_1)+0.39(8a_1^{-2}18a_1)+0.39(8a_1^{-2}12a_1)$
···	7	26.13	0.004	$^2A_1$	$0.42(8a_1^{-1}16a_15e^{-1})+0.30(8a_1^{-1}14a_15e^{-1})$
		26.29	0.004	$^2A_1$	$0.46(8a_1^{-2}10e)-0.30(8a_1^{-2}7e)$
		26.34	0.007	$^2A_1$	$0.44(5e^{-1}9e8a_1^{-1})+0.44(5e^{-2}9e)$
		26.48	0.021	$^2A_1$	$0.30(8a_1^{-1}16a_15e^{-1})$
		26.60	0.055	$^2A_1$	$0.32(5e^{-2}13e)+0.31(5e^{-2}9e)-0.30(8a_1^{-1}11e5e^{-1})$
···	8	26.75	0.009	^2E	$0.31(5e^{-2}12e)$
		26.90	0.027	$^2A_1$	$0.49(8a_1^{-2}11a_1)+0.42(8a_1^{-2}14a_1)-0.31(8a_1^{-2}16a_1)$
		27.05	0.003	$^2A_1$	$0.37(5e^{-2}12e)+0.30(8a_1^{-1}13a_15e^{-1})$
		27.11	0.009	$^2A_1$	$0.55(8a_1^{-2}10a_1)-0.44(8a_1^{-2}6e)$
		27.12	0.009	$^2A_1$	$0.57(8a_1^{-2}6e)+0.40(8a_1^{-2}10a_1)$
		27.31	0.004	^2E	$0.60(8a_1^{-1}13a_15e^{-1})+0.40(8a_1^{-1}10a_15e^{-1})-0.35(8a_1^{-1}17a_15e^{-1})-0.33(5e^{-1}13a_18a_1^{-1})$
···	9	28.73	0.004	$^2A_1$	$0.40(8a_1^{-1}10e5e^{-1})+0.36(8a_1^{-1}10e5e^{-1})-0.35(5e^{-1}10e8a_1^{-1})-0.33(5e^{-1}10e8a_1^{-1})$
		29.07	0.005	$^2A_1$	$0.36(5e^{-2}13e)-0.33(5e^{-2}13e)$
		29.34	0.004	$^2A_1$	$0.51(8a_1^{-1}8e5e^{-1})-0.44(8a_1^{-1}11e5e^{-1})-0.41(5e^{-1}11e8a_1^{-1})-0.37(8a_1^{-1}13e5e^{-1})$ $-0.34(5e^{-1}7e8a_1^{-1})-0.31(5e^{-1}13e8a_1^{-1})-0.30(8a_1^{-1}7e5e^{-1})-0.30(5e^{-1}8e8a_1^{-1})$
		29.48	0.004	$^2A_1$	$0.44(8a_1^{-1}11a_15e^{-1})-0.30(8a_1^{-1}16a_15e^{-1})+0.30(8a_1^{-1}8e5e^{-1})$
		29.70	0.003	$^2A_1$	$0.33(5e^{-2}9e)$
···	10	30.63	0.005	$^2A_1$	$0.29(8a_1^{-1}9e5e^{-1})+0.27(8a_1^{-1}9e5e^{-1})$
		30.65	0.004	$^2A_1$	$0.30(5e^{-2}16a_1)+0.30(5e^{-2}16a_1)$
		31.18	0.004	$^2A_1$	$0.44(5e^{-1}14e8a_1^{-1})+0.41(8a_1^{-1}14e5e^{-1})+0.32(5e^{-1}14e8a_1^{-1})-0.31(5e^{-1}9e8a_1^{-1})$
···	11	32.16	0.005	$^2A_1$	$0.25(5e^{-2}13a_1)+0.24(5e^{-2}7e)+0.23(5e^{-2}13a_1)$
		32.35	0.004	$^2A_1$	$0.40(8a_1^{-2}19a_1)+036(5e^{-2}10e)$

[a]Reference 1.

shake-up states are also due to the two-electron processes including excitations to the Rydberg orbitals.

IV. CONCLUSION

The outer- and inner-valence ionization spectra of the group V hydrides, NH_3, PH_3, and AsH_3, were studied using the extensive and flexible basis sets. The SAC-CI general-*R* method quite accurately reproduced the experimental spectra of these hydrides and gave detailed assignment of the satellite states.

In the outer-valence region of these hydrides, we calculated two main peaks and well reproduced the experimental IPs.

In the inner-valence region, the SAC-CI general-*R* method gave very accurate theoretical spectrum for these hydrides. Several unknown satellite peaks were predicted and the detailed characterizations were given. Our results show that numerous shake-up states exist with distributed intensities in the inner-valence spectrum, especially in the high-energy region, and they constitute several bands that were experimentally resolved. This picture was less clear in the previous theoretical studies. In particular, we calculated detailed spectrum of the shake-up states including Rydberg excitations, for which sufficient Rydberg functions should be included and numerous states should be solved in the calculations.

For NH_3, the SAC-CI spectrum with Gaussian convolution simulated the experimental EMS spectrum quite precisely. We interpreted the spectrum with the calculated peak positions and relative intensities, and further proposed three satellite bands at about 24, 34.5, and 38.5 eV, which have not been definitely analyzed by the EMS and MR-SDCI work. A satellite state at 24 eV corresponds to the ''shake-down''

peak, which has been observed for group V hydrides. Third band was proposed to be constituted by two bands. For PH_3, we reproduced the fine details of the complicated spectrum in the inner-valence region and performed the quantitative analysis. While bands 2 and 3 were assigned as the outer-valence satellite states by SRPES, we suggested that they are dominantly due to the $^2A_1$ inner-valence satellite states, in accordance with the EMS. For AsH_3, we proposed the detailed theoretical spectrum, which was similar to that of PH_3. In the energy region below the strong peak of PH_3 and AsH_3, no ''shake-down'' peak was calculated, but the outer-valence satellite state with ^2E symmetry was calculated with a very weak intensity. Considerable mixing of the two-electron processes with the excitation to Rydberg orbitals was found for these hydrides and we found that the Rydberg basis functions are quite important, especially in the higher energy region.

ACKNOWLEDGMENTS

This study has been supported by the special fund from the Ministry of Education, Science, Culture, and Sports, and a grant from the Kyoto University VBL project.

[1] A. W. Potts and W. C. Price, Proc. R. Soc. London, Ser. A **326**, 181 (1972).
[2] D. W. Turner, C. Baker, A. D. Baker, and C. R. Brundle, *Molecular Photoelectron Spectroscopy* (Wiley, New York, 1970).
[3] W. Domcke, L. S. Cedermaum, J. Schirmer, W. von Niessen, and J. P. Maier, J. Electron Spectrosc. Relat. Phenom. **14**, 59 (1978).
[4] M. S. Banna, H. Kossmann, and V. Schmidt, Chem. Phys. **114**, 157 (1987).
[5] C. Cauletti, M. N. Piancastelli, and M. Y. Adam, J. Mol. Struct. **174**, 135 (1988).
[6] C. Cauletti, M. Y. Adam, and M. N. Piancastelli, J. Electron Spectrosc. Relat. Phenom. **48**, 379 (1989).
[7] A. O. Bawagan, R. Muller-Fiedler, C. E. Brion, E. R. Davidson, and C. Boyle, Chem. Phys. **120**, 335 (1988).
[8] S. A. C. Clark, C. E. Brion, E. R. Davidson, and C. Boyle, Chem. Phys. **136**, 55 (1989).
[9] S. T. Hood, A. Hamnett, and C. E. Brion, Chem. Phys. Lett. **39**, 252 (1976).
[10] A. Hamnett, S. T. Hood, and C. E. Brion, J. Electron Spectrosc. Relat. Phenom. **11**, 263 (1977).
[11] A. Lisini, M. Brosolo, P. Decleva, and G. Fronzoni, J. Mol. Struct.: THEOCHEM **253**, 333 (1992).
[12] G. Fronzoni, G. De Alti, P. Decleva, and A. Lisini, J. Electron Spectrosc. Relat. Phenom. **58**, 375 (1992).
[13] I. Cacelli, R. Moccia, and V. Carravetta, Chem. Phys. **71**, 199 (1982).
[14] G. Bieri, L. Asbrink, and W. von Niessen, J. Electron Spectrosc. Relat. Phenom. **27**, 129 (1982).
[15] W. Domcke, L. S. Cedermaum, J. Schirmer, W. von Niessen, and J. P. Maier, J. Electron Spectrosc. Relat. Phenom. **14**, 59 (1978).
[16] M. Brosolo, P. Decleva, G. Fronzoni, and A. Lisini, J. Mol. Struct.: THEOCHEM **262**, 233 (1992).
[17] H. Nakatsuji and K. Hirao, J. Chem. Phys. **68**, 2053 (1978).
[18] H. Nakatsuji, Chem. Phys. Lett. **59**, 362 (1978); **67**, 329 (1979); **67**, 334 (1979).
[19] H. Nakatsuji, Acta Chim. Hung. **129**, 719 (1992); *Computational Chemistry-Review of Current Trends* (World Scientific, Singapore, 1997), Vol. 2. pp. 62–124.
[20] H. Nakatsuji and K. Hirao, Chem. Phys. Lett. **79**, 292 (1981).
[21] H. Nakatsuji, Chem. Phys. **75**, 425 (1983).
[22] H. Nakatsuji, O. Kitao, and T. Yonezawa, J. Chem. Phys. **83**, 723 (1985).
[23] H. Nakatsuji and S. Saito, J. Chem. Phys. **91**, 6205 (1989); H. Nakatsuji, M. Ehara, M. H. Palmer, and M. F. Guest, *ibid.* **97**, 2561 (1992); H. Nakatsuji and M. Ehara, *ibid.* **101**, 7658 (1994); H. Nakatsuji, J. Hasegawa, and M. Hada, *ibid.* **104**, 2321 (1996).
[24] M. Ehara, Y. Ohtsuka, and H. Nakatsuji, Chem. Phys. **104**, 113 (1998).
[25] H. Nakatsuji, Chem. Phys. Lett. **177**, 331 (1991).
[26] H. Nakatsuji, J. Chem. Phys. **83**, 713 (1985); **83**, 5743 (1985); **94**, 6716 (1991).
[27] M. Ehara, M. Ishida, K. Toyota, and H. Nakatsuji, *Reviews in Modern Quantum Chemistry*, edited by K. D. Sen (World Scientific, Singapore, submitted).
[28] M. Ehara and H. Nakatsuji, Chem. Phys. Lett. **282**, 347 (1998); Spectrochim. Acta, Part A **55**, 487 (1999).
[29] J. Hasegawa, M. Ehara, and H. Nakatsuji, Chem. Phys. **230**, 23 (1998).
[30] M. Ehara, P. Tomasello, J. Hasegawa, and H. Nakatsuji, Theor. Chem. Acc. **102**, 161 (1999).
[31] M. Ehara, M. Ishida, and H. Nakatsuji, J. Chem. Phys. **114**, 8990 (2001).
[32] K. P. Huber and G. Herzberg, *Molecular Spectra and Molecular Structure, IV. Constants of Diatomic Molecules* (Van Nostrand, New York, 1979).
[33] J. H. Callomon, E. Hirota, K. Kuchitu, W. J. Lafferty, A. G. Maki, and C. Bornstein, *New Series, Group II* (Springer, Berlin, 1976).
[34] A. Schafer, H. Horn, and R. Ahlrichs, J. Chem. Phys. **97**, 2571 (1992).
[35] T. H. Dunning, Jr., J. Chem. Phys. **90**, 1007 (1989).
[36] D. E. Woon and T. H. Dunning, Jr., J. Chem. Phys. **98**, 1358 (1993).
[37] S. Süzer, S. T. Lee, and D. A. Shirley, Phys. Rev. A **13**, 1842 (1976).
[38] R. I. Martin and D. A. Shirley, J. Chem. Phys. **64**, 3685 (1976).
[39] M. J. Frisch, G. W. Trucks, H. B. Schlegel *et al.*, GAUSSIAN 98, Revision A.5, Gaussian, Inc., Pittsburgh, PA, 1998.
[40] H. Nakatsuji, M. Hada, M. Ehara, J. Hasegawa, T. Nakajima, H. Nakai, O. Kitao, and K. Toyota, SAC/SAC-CI program system SAC-CI96 for calculating ground, excited, ionized, and electron-attached states having singlet to septet spin multiplicities, 1996.
[41] F. H. Dorman and J. D. Morrison, J. Chem. Phys. **35**, 575 (1961).
[42] D. M. Chipman, J. Electron Spectrosc. Relat. Phenom. **14**, 323 (1987).
[43] M. Y. Adam, C. Cauletii, and M. N. Plancastelli, J. Electron Spectrosc. Relat. Phenom. **42**, 1 (1987).